ABUAD Journal of Engineering Research and Development (AJERD)
ISSN (online): 2645-2685; ISSN (print): 2756-6811

Volume 8, Issue 1, 315-323

Semi Empirical Modelling of Alkaline Water Electrolysis Green Hydrogen Using Biosynthesized Lye and Caustic Soda Electrolytes

Anthony Owoicho IJIGA[1], Sylvia IGBAFE[1], Akeem Aderibigbe ADEBOMEHIN[2], Anselm Iuebego IGBAFE[1]

[1]*Department of Chemical and Petroleum Engineering, Afe Babalola University, Ado-Ekiti, Ekiti State, Nigeria*
aoijiga007@gmail.com/igbafesylvia@gmail.com/igbafeai@abuad.edu.ng

[2]*Artificial Intelligence and Software Development Research, Air Force Research and Development Institute, Osogbo, Osun State, Nigeria*
aakeem2@gmail.com

Corresponding Author: igbafeai@abuad.edu.ng, +234-806-659-6180

Date Submitted: 15/08/2024
Date Accepted: 26/03/2025
Date Published: 29/04/2025

***Abstract**: Semi empirical modelling of an alkaline water electrolysis system for green hydrogen production was carried out in this paper. Green hydrogen which is an alternative to fossil fuels and other sources of energy because of its renewability and sustainability is produced via alkaline water electrolysis utilizing biosynthesized lye (KOH) and caustic soda (NaOH) obtained from charring unripe plantain peel and electrolysing sea water respectively. The alkaline water electrolysis process was carried out at electrolyte concentrations of 25 g/L, 30 g/L and 35g/L for KOH and NaOH, at temperatures 45 ^oC, 55 ^oC, 65 ^oC, 75 ^oC and 85 ^oC, applying a voltage of 9 volts and running the electrolytic process for 15 minutes to obtain the volume of hydrogen generated at the cathode. The models developed were for the cell voltage of the energy consumed, the Faraday's efficiency of the alkaline water electrolysis and the gas purity of the hydrogen produced. All R^2 values which represent the coefficient of determination were within the range of 0.96-0.999, indicating that the semi empirical models were a good fit to represent the alkaline water electrolysis, with the exception with the cell voltage models at 30 g/L of KOH and 30 g/L NaOH which had an R^2 values of 0.7826 and 0.782 respectively. Also, a pop and combustion test was carried out to determine the presence and flammability of hydrogen at the cathode of the electrolytic cell.*

***Keywords**: Semi Empirical Modelling, Alkaline Water Electrolysis, Green Hydrogen, Biosynthesized Lye, Caustic Soda*

1. INTRODUCTION

With the increasing demand for energy, the search for alternative and environmentally friendly sources of energy has gained prominence. The reliance on fossil fuels not only contributes to environmental degradation but also engenders geopolitical and economic challenges owing to the volatile nature of fossil fuel prices and the finite nature of these resources further underscore the fragility of the current energy paradigm [1-3]. This search has led to the interest in hydrogen as a necessary alternative. Unlike conventional fuels, hydrogen combustion produces water vapor as its only byproduct, eliminating the release of harmful pollutants [4]. This intrinsic green-energy characteristic positioned hydrogen as a key player in the transition towards a sustainable energy future. Harnessing hydrogen as a fuel source holds the potential to mitigate environmental impacts, reduce dependence on fossil fuels, and foster a more resilient and sustainable energy ecosystem [5]. It is however important to produce hydrogen without adverse effect to the environment. Grey hydrogen is produced through the traditional method of steam methane reforming or gasification of coal, which involves extracting hydrogen from natural gas or coal. During these processes, carbon dioxide (CO_2) is emitted as a byproduct, contributing to greenhouse gas emissions [6]. In the blue hydrogen process, CO_2 emissions generated during hydrogen production are captured and stored underground, preventing them from entering the atmosphere. This approach addresses the greenhouse gas emissions associated with grey hydrogen, making blue hydrogen a transitional solution toward cleaner hydrogen production [6]. However, green hydrogen is considered the most environmentally friendly option as it is produced through electrolysis using renewable energy sources, such as solar, wind, or hydropower. In this process, water is split into hydrogen and oxygen using electricity generated from renewable sources, with zero direct emissions of greenhouse gases. Green hydrogen holds immense promise for a sustainable energy future, aligning closely with the global transition to decarbonize industries and reduce dependence on fossil fuels However; green hydrogen is challenged by its scalability and cost competitiveness of the particular green hydrogen process [7]. Different green hydrogen methods are however available. The proton exchange membrane (PEM) which uses a solid polymer electrolyte membrane, typically made of a proton-conducting polymer such as Nafion. The solid oxide electrolysis (SOE) which involves the use of a solid ceramic electrolyte typically made of zirconia or ceria. The alkaline water electrolysis (AWE) which involves the use of an alkaline electrolyte solution, typically potassium hydroxide (KOH) or sodium hydroxide (NaOH). This solution facilitates the ionization of water molecules, allowing the release of hydrogen and oxygen gases at the cathode and anode, respectively [7]. The AWE is adopted for green hydrogen due to its cheap raw materials which are water, KOH and NaOH. The paper presents the numerical semiempirical modelling of AWE with alkaline derived from extremely cheap and sustainable KOH and NaOH resources of biochar produced from unripe plantain peel and electrolysis of sea water respectively [8-10].

1.1 Model

Semi empirical model was developed to evaluate the performance of the alkaline electrolysis system set up. The model components include the cell voltage, Faraday's efficiency and gas purity.

1.2 Cell Voltage Submodel

This model predicts the electric potential difference between the two electrodes of an electrochemical cell, known as the cell potential. The cell voltage model describes the behaviour of an electrolyser and takes into account the effects of temperature and current density on the cell potential. In theory, the cell voltage model or cell potential model by Nernst model equation can be parametrised as shown in Equation (1) reduced and modified for reaction temperatures and system current densities [11-13].

$$U_{cell} = [(r_1 + d_1) + r_2 T + d_2 P] \times i + s \tag{1}$$

Where T is operating temperature (^{o}C) and i is the current density (A/cm^2). Using the Microsoft excel solver, the constants, r_1, r_2, d_1, d_2 and s in Equations (1) were determined across 45 to 85 ^{o}C reaction temperatures for each measured current divided by the electrode's cross-sectional area.

1.3 Faraday Efficiency Submodel

The amount of gas produced in an electrochemical process is directly related to the electric charge used by the cell, according to Faraday's law. In an ideal water electrolysis system, the electric charge passing through the cell corresponds directly to the amount of hydrogen generated [13]. This relationship allows for the assessment of the process efficiency by comparing the supplied charges to the system with the actual amount of hydrogen produced [14]. The efficiency, known as Faraday's efficiency, is calculated as the ratio of the volume of gas produced to the theoretical volume of gas that should have been produced at the same time, as shown in Equation (2), [15].

$$N_f = \frac{192970 \, x \, V_{exp}}{i \, x \, V_m \, x \, t} \tag{2}$$

Where V_{exp} is the experimental volume, i is the current density passes through the cell during a period (t), V_m is the molar volume of ideal gas under standard conditions. Empirically, the Faraday efficiency can be modelled using an empirical five-parameter model [11, 16] given by Equation (3).

$$N_f = B_1 + B_2 \, e^{\frac{(B_3 + B_4 T + B_5 T^2)}{i}} \tag{3}$$

Where B_1, B_2, B_3, B_4, B_5 are constants computed using Microsoft excel solver.

1.4 Gas Purity Submodel

In the production of hydrogen from water, a phenomenon known as gas crossover is experienced. Gas crossover results in the contamination of the product gases at the electrodes. Although with poor solubility of the gases in water, contamination could arise from the dissolution of small amounts of hydrogen and oxygen gases into the liquid electrolyte. It is important to note that the gas separator vessel can only remove gas bubbles and not the dissolved gases in the electrolyte [16,17]. According to Sanchez *et al*. (2018), the gas purity can be modelled using Equation (4).

$$HTO = C_1 + C_2 T + C_3 T^2 + (C_4 + C_5 + C_6 T^2) \, e^{\frac{(C_7 + C_8 T + C_9 T^2)}{i}} \tag{4}$$

Where C_1, C_2, C_3, C_4, C_5, C_6, C_7, C_8, C_9 are constants computed using Microsoft excel solver.

2. MATERIALS AND METHOD

2.1 Experimental

The chemical reagents used in this study are distilled water, sodium hydroxide pellets and potassium hydroxide pellets. The equipment used is electronic weigh balance, water bath, multimeters, copper electrodes and a variable DC source.

2.2 Preparation of Biolye Electrolyte

The process of preparation KOH involves the use of plantain peels due to the presence of potassium. The plantain peels utilised in the project were gathered from the wastes of Afe Babalola University Ado-Ekiti (ABUAD) hostels. Following the gathering of plantain peels, they were chopped into smaller pieces and cleaned with distilled water to get rid of any dirt that was on them. Then they were dried in an oven at 150 ^{o}C for 4 hours. The dried plantain peels were pulverized and sieved using the mesh size of 200 micron. The powdered peels were then heated in an open but controlled environment to produce biochar which is then dissolved in 250 ml of distilled water to form solution. The solution is then filtered the filtrate is allowed to crystallize for a day. The procedure was adapted and modified from [8,10,18].

The process of preparing NaOH from seawater via electrolysis involves the use of two containers one filled 100 ml of distilled water and the other 100 ml of sea water. The containers are connected using a salt bridge and copper electrodes placed in both and these electrodes are connected to a DC source of 12 volts. The voltage causes the sodium chloride present in sea water to break down into its constituent elements, sodium (Na) and chlorine (Cl). The sodium ions combine with water molecules to form sodium hydroxide (NaOH) solution. The procedure was adapted and modified from [9].

2.3 Preparation of Caustic Soda Electrolyte

Standard solutions of potassium hydroxide and sodium hydroxide were prepared at various concentration. The first concentration that was prepared was 35 g/L of KOH which was made by weighing 7 g of potassium hydroxide and dissolving it in 200 ml of distilled water and stirring in a beaker until completely dissolved. Then 30 g/L of potassium hydroxide was prepared by weighing 6 g of potassium hydroxide and dissolving it in 200 ml of distilled water and stirring in a beaker until completely dissolved. 25 g/L of potassium hydroxide was prepared by weighing and 5 g of potassium hydroxide, dissolving it in 200 ml of distilled water and stirring in a beaker until completely dissolved. This same preparation was used for sodium hydroxide (NaOH) [9,18].

2.4 Electrolytic Cell Design

The experimental was carried out with the use of an electrolytic cell. The electrolytic cell was constructed using a plastic container, two 100 ml measuring cylinder and two copper electrodes of 5mm in diameter and 130mm in length and solutions of various concentrations KOH and NaOH were used as electrolytes. A variable DC source was connected to both ends of the electrode. Two multimeters were connected in series to the electrolytic cell to measure the current and voltage applied to the system. Both electrodes are kept at the opposite sides of the plastic container and the distance between the electrodes was maintained. The gases produced at the anode and cathode are collected separately by the two measuring cylinders on top of the electrodes (Figure 1a-c). The volume of hydrogen produced can be measured by down displacement of the water within the measuring cylinder [19].

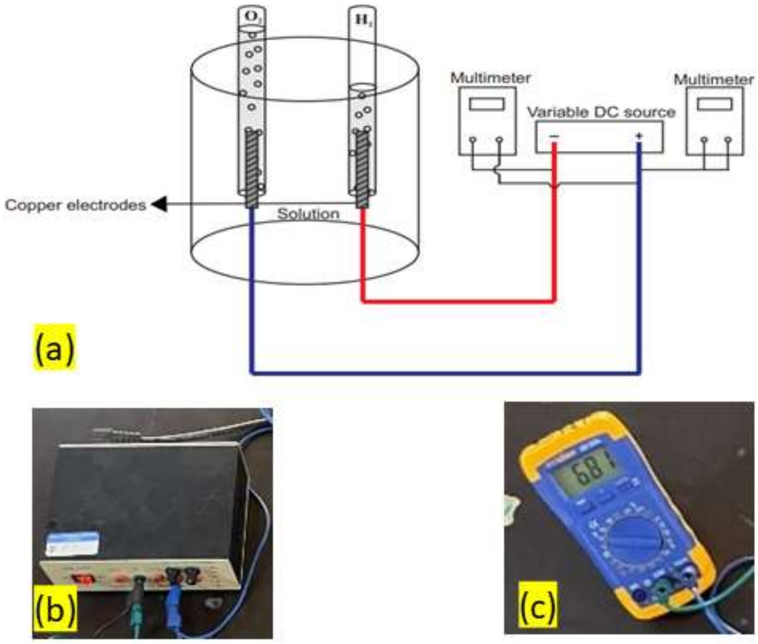

Figure 1: (a) Experimental setup for electrolysis, (b) Variable-DC power source, (c): Multimeter

3. RESULTS AND DISCUSSION

3.1 Test of Hydrogen Gas Produced

The pop test is a qualitative method used for assessing the purity and flammability of generated hydrogen gas. An ignited flame was brought in close contact with the cathode and a pop sound was heard to confirm the presence of hydrogen and upon further contact combustion was sustained.

3.2 Effect of Temperature and Electrolyte Concentrations on Volume of Produced Hydrogen

The effects of varying temperature and electrolyte concentration on the volume of hydrogen gas produced at the cathode are shown in the Figures 2a and 2b. With increased KOH concentration, the volume of hydrogen gas generated at the cathode decrease with an increase in temperature. The solution with 35 g/L KOH gives the best outcome in terms of volume generated throughout the range of operating temperature for a fixed time of 15 minutes. This could be as a result of the electrodes' conductance and the electrolyte's concentration, which control the rate at which current flows and, in turn, raise the effective ion collision rate. Similarly, for concentrations of NaOH, the volume of hydrogen gas generated decreases with an increase in temperature and the solution with 35 g/L NaOH gives the best outcome in terms of volume generated throughout the range of operating temperature.

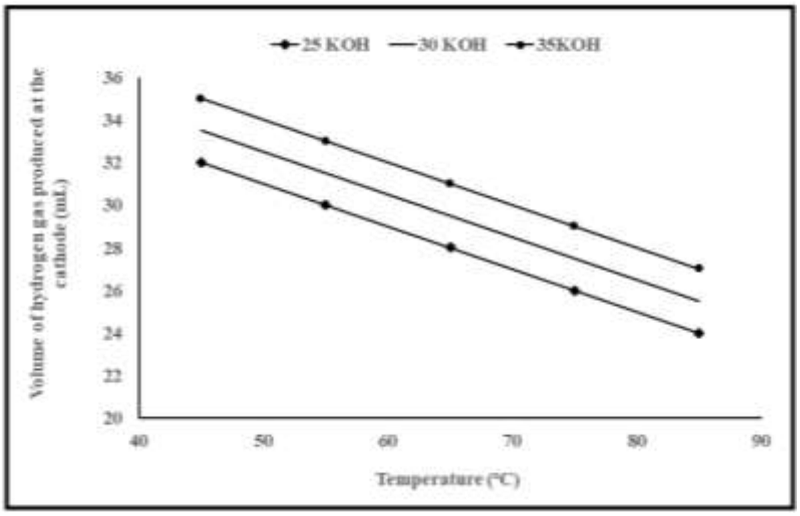

Figure 2a: Volume of gas produced at cathode versus temperature at different concentrations of KOH electrolyte

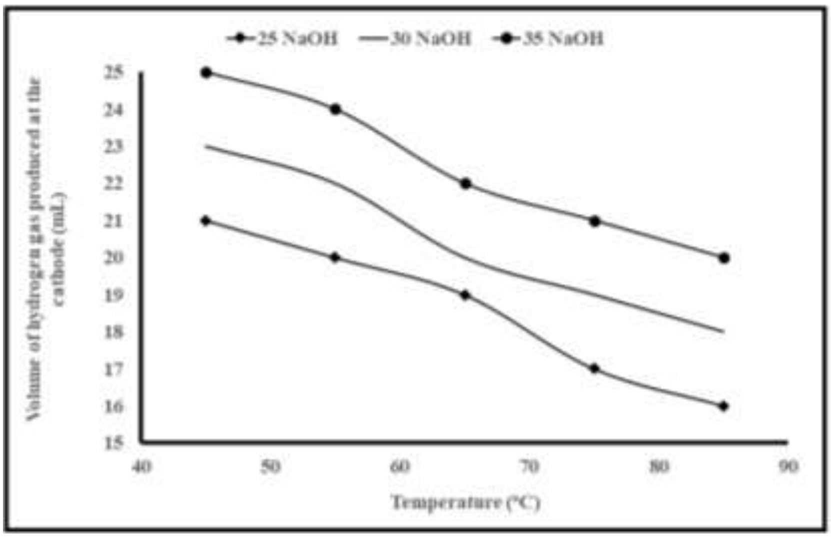

Figure 2b: Volume of gas produced at cathode versus temperature at different concentrations of NaOH electrolyte

3.3: Effect of Temperature on Cell Voltage

Cell voltage is independent of electrolyte concentration. Therefore, the relationship between the experimental electrolyser cell voltage and operating temperature for the optimum electrolyte concentration of 30 g/L is shown in the Figures 3a and 3b. For 30 g/L KOH there is a decrease in cell voltage with an increase in operating temperature. This trend is also noticed for 30 g/L NaOH electrolyte concentration. This may be attributed to enhance reaction kinetics and reduction in reversible voltage, causing the required energy to decrease as temperature rises. Since low energy demands are advantageous, the temperature 85°C yields the best cell voltage of 1.144 V for 30 g/L electrolyte concentration.

3.4 Parametrisation of Cell Voltage Submodel

The cell voltage or cell potential difference defines the observed consumption by the cell during operation. The model coefficients for the alkaline water electrolysis study with 30 g/L KOH and 30 g/L NaOH electrolyte were computed using Microsoft excel solver and then substituted into Equation 1 to obtain the modelled cell voltage

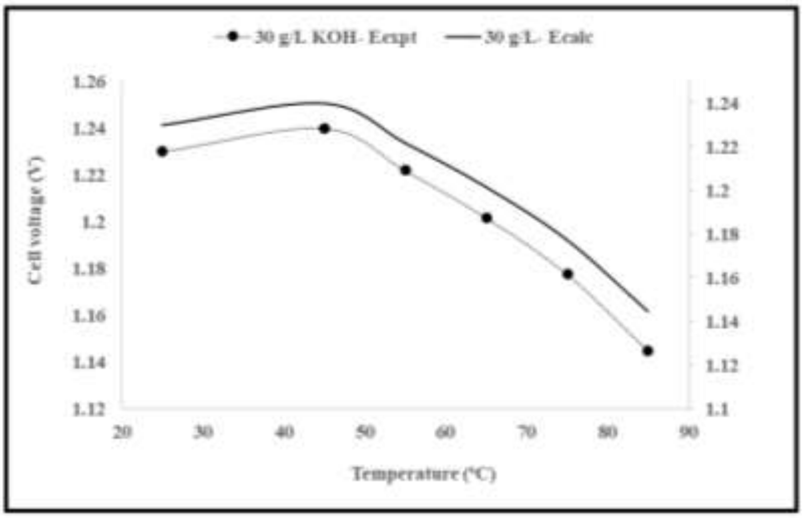

Figure 3a: Effects of modelled and experimental cell voltage versus temperature at 30 g/L KOH electrolyte concentration

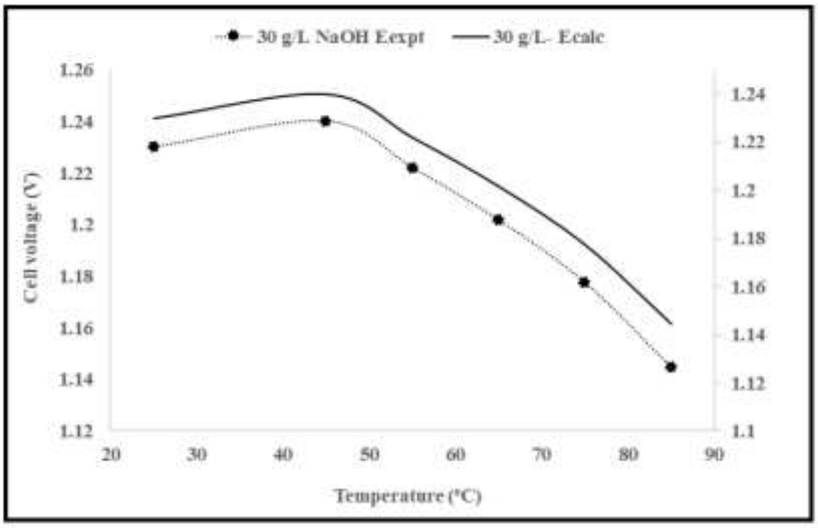

Figure 3b: Effects of modelled and experimental cell voltage versus temperature at 30 g/L NaOH electrolyte concentration

Table 1: Parameterised cell voltage model constant at varying electrolyte concentrations

Coefficient	Unit	30 g/L KOH	30 g/L NaOH
r_1	$\Omega\ m^2$	-0.665957235	-0.6659572
r_2	$\Omega\ m^2\ {}^oC^{-1}$	-3.36759E-16	-2.5951E-16
d_1	$\Omega\ m^2$	0.33297345	0.332973485
d_2	$\Omega\ m^2\ bar^{-1}$	0.332983026	0.332983061
S	V	0.000502676	0.000466771

3.5 Cell Voltage Submodel Validation

The submodel verification are also displayed in the plots of experimental and calculated over the operating temperature range for 30 g/L KOH and 30 g/L NaOH electrolyte concentrations. This was done since 30 g/L KOH and 30 g/L NaOH electrolyte concentrations yielded the optimal operating electrolyte concentrations and cell voltages is unaffected by varying electrolyte concentrations [20]. In the range of operating temperatures, the submodel with KOH gave R^2 of 1.0 indicating an outstanding fit of the submodel. Similarly, with NaOH electrolyte concentration, an R^2 of 99.62 obtained also specifies an excellent prediction if applied.

3.6 Effect of Temperature and Electrolyte Concentration on Faraday's Efficiency

The Faraday's efficiency which describes the efficiency of an electrochemical reaction, specifically the potential of a system with respect to the amount of current entering into the system. The relationship between faraday's efficiency, electrolyte concentration and operating temperature is shown in Figures 4a and 4b. All the electrolyte concentrations exhibited a decline in Faraday number efficiency with increasing temperature. This trend is applicable to both concentrations of KOH and NaOH. Although, for 25 g/L NaOH there was an increase in faraday's efficiency for an increase in temperature from 45-55 °C but as the temperature continued to increase, the decline in faraday's efficiency followed.

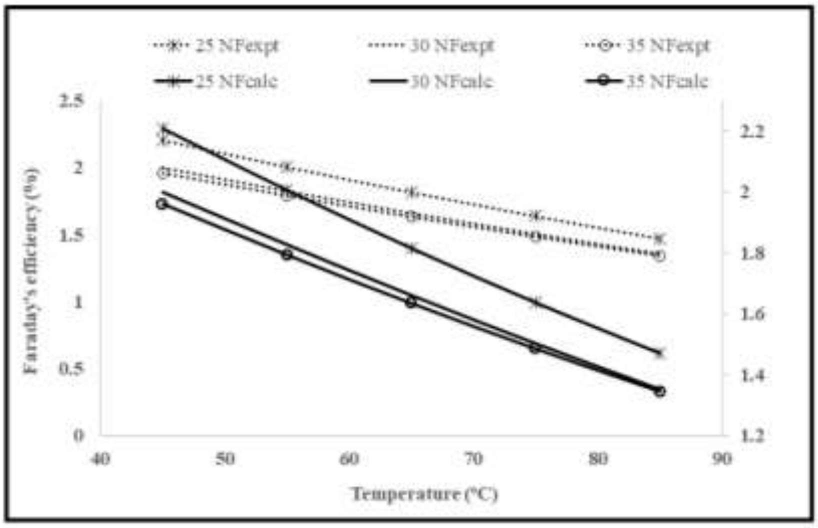

Figure 4a: Effects of modelled and experimental Faraday's efficiency versus temperature at varying KOH electrolyte concentrations

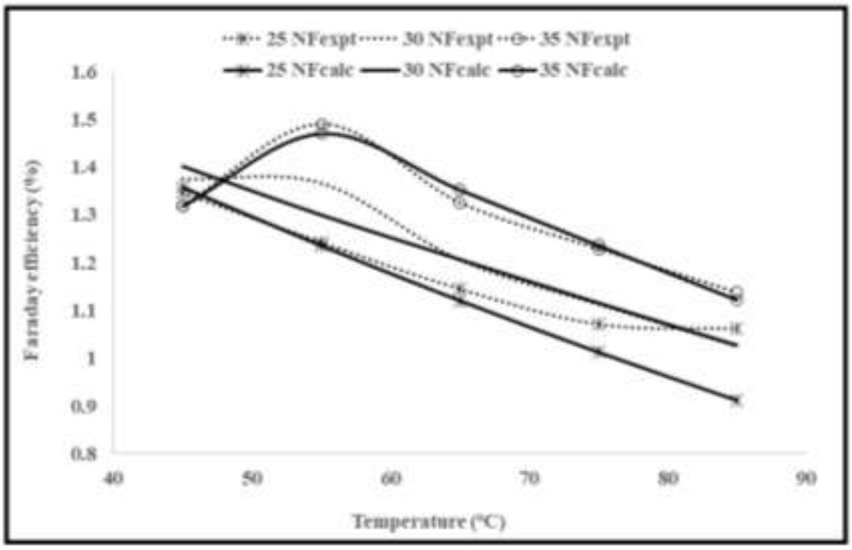

Figure 4b: Effects of modelled and experimental Faraday's efficiency versus temperature at varying NaOH electrolyte concentrations

3.7 Parametrisation of Faraday's efficiency submodel

The model coefficients for Faraday's efficiency for this alkaline water electrolysis with 25 g/L 30 g/L and 35 g/L of KOH and NaOH electrolyte concentrations computed using Microsoft excel solver and these coefficients are substituted into Equation (3) to obtain the modelled Faraday efficiency.

Table 2: Parameterised Faraday's efficiency model constants at varying KOH electrolyte concentrations

Coefficient	Unit	25 g/L KOH	30 g/L KOH	35 g/L KOH
B_1	-	3.369681304	1.229538742	3.077933449
B_2	-	3.360787581	1.232621769	3.077933449
B_3	$A\ m^2$	0.009703227	0.008673378	0.007719739
B_4	$A\ m^2\ {}^oC^{-1}$	1.582069741	5.704642503	1.302286458
B_5	$A\ m^2\ {}^oC^{-2}$	-0.012268934	-0.019501607	-0.013308027

Table 3: Parameterised Faraday’s efficiency model constants at varying NaOH electrolyte concentrations

Coefficient	Unit	25 g/L NaOH	30 g/L NaOH	35 g/L NaOH
B_1	-	2.094837459	0.651466553	0.206645172
B_2	-	2.09172836	0.855984048	0.348209002
B_3	$A\ m^2$	0.009009681	0.028532541	0.058519035
B_4	$A\ m^2\ {}^oC^{-1}$	1.516384989	4.528082565	9.945478508
B_5	$A\ m^2\ {}^oC^{-2}$	-0.012709351	-0.014780995	-0.023852534

3.8 Faraday’s Efficiency Submodel Validation

Within the temperature range, the model adequately reproduced the Faraday’s efficiency pattern of this alkaline electrolytic cell with a coefficient of determination (R^2) of 0.9985 for 25 g/L KOH. At the same temperature conditions but at 30 g/L KOH electrolyte concentration, the model gave an R^2 of 0.9993. At the same temperature conditions but with 35 g/L KOH electrolyte concentration, an R^2 of 0.9988 was achieved also indicating a good fit. Similarly, with a concentration of 25 g/ L NaOH, the model gave an R^2 of 0.9986, at 30 g/L NaOH, the model gave an R^2 of 0.993 and at 35 g/L NaOH, the model gave an R^2 of 0.5799. Therefore, the likelihood of a better prediction of the Faraday’s efficiency number is at electrolyte concentration of 30 g/L.

3.9 Effect of temperature and electrolyte concentration on gas purity

The effect of temperature and electrolyte concentration on the purity of hydrogen gas produced at the cathode against oxygen gas contaminations is shown in Figures 5a and 5b. With increasing concentrations of KOH, the HTO decreases with an increase in operating temperature indicating an increase in gas purity. Also, the concentration 30 g/L KOH gives the least HTOs indicating that 30 g/L as the best operating temperature. Similarly, for increasing concentrations of NaOH, the HTO decreases with an increase in operating temperature indicating an increase in gas purity.

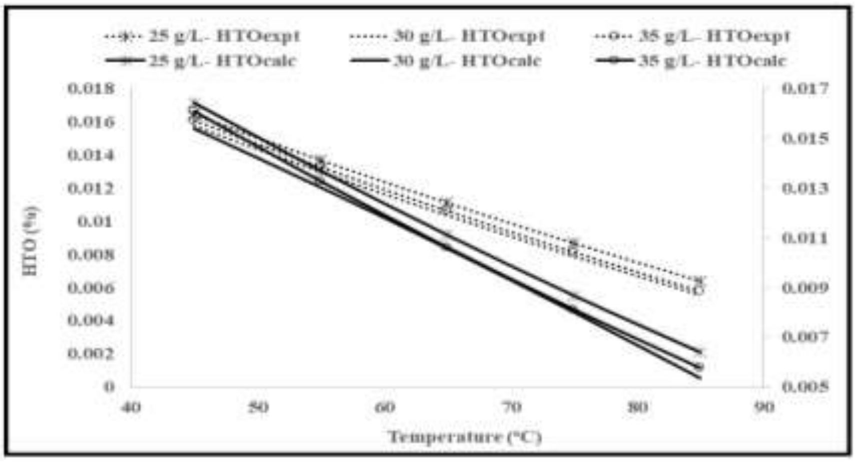

Figure 5a: Effects of modelled and experimental Hydrogen to oxygen (HTO) versus temperature at varying KOH electrolyte concentrations

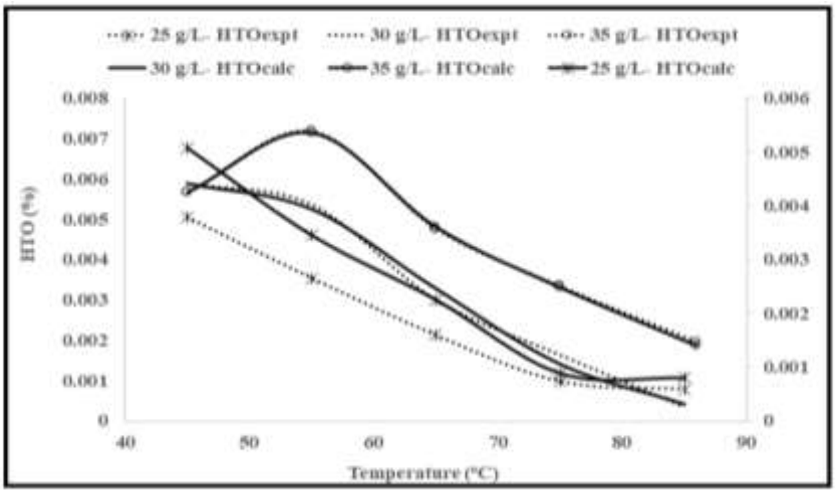

Figure 5b: Effects of modelled and experimental Hydrogen to oxygen (HTO) versus temperature at varying NaOH electrolyte concentrations

3.10 Parametrisation of Gas Purity Submodel

The gas purity model coefficients are computed using Microsoft excel solver and substituted into equation (4) to obtain the modelled gas purity model for this study of alkaline water electrolysis with 25 g/L, 30 g/L and 35 g/L of KOH and NaOH electrolyte concentrations.

Table 4: Parameterised gas purity model constants at varying KOH electrolyte concentrations

Coefficient	Unit	25 g/L KOH	30 g/L KOH	35 g/L KOH
C_1	-	0.030481716	0.024739672	-0.055042281
C_2	$^oC^{-1}$	-0.000346327	-0.000184715	-0.011202681
C_3	$^oC^{-2}$	7.4022E-07	-5.11123E-07	-0.002500237
C_4	-	0.570095733	-363.3248446	0.084505371
C_5	$^oC^{-1}$	-1640.847912	-140690.3251	0.010927632
C_6	$^oC^{-2}$	-588873.1465	-11957670.8	0.002498681
C_7	$A\ m^{-2}$	-2984.742701	-53056.54105	2.51673E-05
C_8	$A\ m^2\ ^oC^{-1}$	-8.911262728	-37.58218114	0.008430178
C_9	$A\ m^2\ ^oC^{-2}$	-84936720.89	-84936720.89	-3.46453E-05

Table 5: Parameterised gas purity model constants at varying NaOH electrolyte concentrations

Coefficient	Unit	25 g/L NaOH	30 g/L NaOH	35 g/L NaOH
C_1	-	-0.431864887	1.09208E-05	1.10455E-05
C_2	$^oC^{-1}$	0.16657679	-0.233824232	0.257190582
C_3	$^oC^{-2}$	-0.000566817	0.008475423	0.006405767
C_4	-	0.56281604	1.09318E-05	1.10587E-05
C_5	$^oC^{-1}$	-0.174595644	0.234666199	-0.25468355
C_6	$^oC^{-2}$	0.000760405	-0.008496934	-0.006469256
C_7	$A\ m^{-2}$	0.036479549	-1.434587209	2.456816637
C_8	$A\ m^2\ ^oC^{-1}$	0.008657443	0.005328456	-0.084898989
C_9	$A\ m^2\ ^oC^{-2}$	1.582069741	-6.50513E-05	0.000300615

3.11 Gas Purity Submodel Validation

The experimental and calculated gas purity values at temperatures of 45 to 85 ^oC and electrolyte concentrations of 25 g/L KOH, the model significantly replicated the behaviour of the alkaline electrolysis with R^2 value of 0.9988 which indicate that the model is a good fit. Under the same temperature conditions but at 30 g/L KOH electrolyte concentration, the model gave an outstanding R^2 value of 0.9994. At the same temperature conditions with 35 g/L KOH electrolyte concentration, an R^2 value of 0.9988 was obtained. Similarly, with a concentration of 25 g/ L NaOH, the model gave an R^2 of 0.9438, at 30 g/L NaOH, the model gave an R^2 of 0.9768 and at 35 g/L NaOH, the model gave an R^2 of 0.7785. Therefore, the likelihood of a better prediction of the gas purity is at electrolyte concentration of 30 g/L.

CONCLUSION

Biosynthesized lye (KOH) and caustic soda (NaOH) were achieved using biochar of unripe plantain peel and the electrolysis of sea water respectively. Both sythesisised alkali formed sustainable resources at concentrations of 25 g/L, 30 g/L and 35 g/L for electrolyte in alkaline water electrolysis process. The electrolysis process yielded hydrogen and oxygen gases at an optimal condition of 15 minutes applying a voltage of 9 volts at 45^oC to 85^oC using the aforementioned electrolyte concentrations. Hydrogen was produced at the cathode of the electrolytic cell and confirmed by the pop and combustion test. The volume of hydrogen produced increase with electrolyte concentration. The highest volume of hydrogen produced was at 35 g/L KOH. The actual cell voltage, Faraday efficiency and gas purity varied inversely with temperature. The optimal cell voltage is 1.5 volts using 35 g/L of either electrolyte (KOH or NaOH) for 15 minutes and at a temperature of 85 ^oC. At these optimal conditions, the corresponding Faraday efficiency is approximately 1.34 % for 35 g/L KOH and 1.14% g/L NaOH. With respect to the gas purity that is the content of hydrogen to oxygen, with 35 g/L KOH is 0.5% and 35 g/L NaOH is 0.2%. The semi empirical model for cell voltage, Faraday efficiency and gas purity developed had accuracy by the coefficient of determination values ranging between 0.96-0.99. The model accurately represents the alkaline water electrolysis at 35 g/L electrolyte concentrations with exception of cell voltage models at 30 g/L of KOH and NaOH which had an R^2 value of 0.79 and 0.78 respectively.

Further research in the future should focus on the following aspects:

(1) Development of renewable and sustainable electrodes against corrosion and other deterioration.
(2) Development of sustainable bio electrocatalyst from biodegradable sources for sustainable environments.

ACKNOWLEDGEMENTS

The founder of Afe Babalola university, Nigeria, Aare Afe Babalola for providing a conducive environment and facilities for advanced studies, and the entire staff of the department of chemical and petroleum engineering for necessary materials used in this study.

Availability of data and materials

The raw data supporting the conclusions of this article can be made available by the authors, without any reservation.

REFERENCES

[1] Martins, F., Felgueiras, C., Smitkova, M.F., & Caetano, N.S. (2019). Analysis of Fossil Fuel Energy Consumption and Environmental Impacts in European Countries, Energies, 12(6): 964-973. https://doi.org/10.3390/en12060964.

[2] Wang, M., Wang, G., Sun, Z., Zhang, Y., & Xu, D. (2019). Review of renewable energy-based hydrogen production processes for sustainable energy innovation, Global Energy Interconnection, 2(5): 436-443. https://doi.org/10.1016/j.gloei.2019.11.019

[3] ul Husnain, M.I., Syed, Q.R., Bashir, A., & Khan, M.A. (2022). Do geopolitical risk and energy consumption contribute to environmental degradation? Evidence from E7 countries, Environmental Science and Pollution Research International, 29(27): 41640–41652. https://doi.org/10.1007/s11356-021-17606-z.

[4] Crabtree, G.W & Dresselhaus, M.S. (2008). The hydrogen fuel alternative, MRS Bulletin, 33(4): 421–428. https://doi.org/10.1557/mrs2008.84.

[5] Nicoletti, G., Arcuri, N., Nicoletti, G., & Bruno, R. (2015). A technical and environmental comparison between hydrogen and some fossil fuels, Energy Conversion and Management, 89: 205–213. https://doi.org/10.1016/j.enconman.2014.09.057.

[6] Saha, P., Akash, F.A., Shovon, S.M., Monir, M.U., Ahmed, M.T., Khan, M.F.H., Sarkar, S.M., Islam, M.K., Hasan, M.M., Vo, D.V.N., & Aziz, A.A. (2023). Grey, blue, and green hydrogen: A comprehensive review of production methods and prospects for zero-emission energy, International Journal of Green Energy, 1-15. https://doi.org/10.1080/15435075.2023.2244583.

[7] Brauns, J & Turek, T. (2020), Alkaline water electrolysis Powered by Renewable Energy: a review, Processes, 8(2): 248. https://doi.org/10.3390/pr8020248.

[8] Enontiemonria, E.V., Abiodun, O.J., & Eric, K.E. (2016). Extraction and use of potassium hydroxide from ripe plantain peels ash for biodiesel production, Journal of Biobased Materials and Bioenergy, 10(1): 1-9. https://doi.org/10.1166/jbmb.2016.1567.

[9] Hou, M., Chen, L., Guo, Z., Dong, X., Wang, Y., & Xia, Y. (2018). A clean and membrane-free chlor-alkali process with decoupled Cl_2 and H_2/NaOH production, Nature communications, 9(1): 438. https://doi.org/10.1038/s41467-018-02877-x

[10] Ofori, P., & Awudza, J.A. (2017). Production of potassium hydroxide (KOH) from plant biomass: the case of cocoa pod husks and plantain peels, Kwame Nkrumah University of Science and Technology, Kumasi.

[11] Ulleberg, O. (2003). Modelling of advanced alkaline electrolyzer: a system simulation approach, International Journal of Hydrogen Energy, 28(1): 21-33. https://doi.org/10.1016/S0360- 3199(02)00033-2.

[12] Diéguez, P.M., Ursúa, A., Sanchis, P., Sopena, C., Guelbenzu, E., & Gandía, L.M. (2008). Thermal performance of a commercial alkaline water electrolyzer: Experimental study and mathematical modelling, International journal of hydrogen energy, 33(24):7338-7354. https://doi.org/10.1016/j.ijhydene.2008.09.051.

[13] Sanchez, M., Amores, E., Rodriguez, L., & Clemente-Jul, C. (2018). Semi-empirical model and Experimental Validation for the Performance Evaluation of a 15kW Alkaline Water Electrolyzer, International Journal of Hydrogen energy, 43(45): 20332-20345. https://doi.org/10.1016/j.ijhydene.2018.09.029.

[14] Bessarabov, D., Wang, H., Li, H & Zhao, N. (2016). PEM electrolysis for hydrogen production: principles and applications. CRC press.

[15] Sellami, M.H., & Loudiyi, K. (2017). Electrolytes behavior during hydrogen production by solar energy, Renewable & Sustainable Energy Reviews, 70: 1331–1335. https://doi.org/10.1016/j.rser.2016.12.034

[16] Hug, W., Bussmann, H., & Brinner, A. (1993). Intermittent operation and operation modelling of an alkaline electrolyser, International journal of hydrogen energy, 18(12): 973-977. https://doi.org/10.1016/0360-3199(93)90078-O.

[17] Haug, P., Koj, M., & Turek, T. (2017). Influence of process conditions on gas purity in alkaline water electrolysis, International Journal of Hydrogen Energy, 42(15): 9406-9418. https://doi.org/10.1016/j.ijhydene.2016.12.111.

[18] Gilliam, R.J., Graydon, J.W., Kirk, D.W., & Thorpe, S.J. (2007). A review of specific conductivities of potassium hydroxide solutions for various concentrations and temperatures, International Journal of Hydrogen Energy, 32(3): 359–364. https://doi.org/10.1016/j.ijhydene.2006.10.062.

[19] Yuvaraj, A.L., & Santhanaraj, D. (2013). A systematic study on electrolytic production of hydrogen gas by using graphite as electrode, Materials Research,17(1): 83–87. https://doi.org/10.1590/S1516-14392013005000153.

[20] Shen, M., Bennett, N., Ding Y., & Scott, K. (2011). A concise model for evaluating water electrolysis, International Journal of Hydrogen Energy,36(3): 14335–14341. https://doi.org/10.1016/j.ijhydene.2010.12.029.